Bone 157 (2022) 116344

Contents lists available at ScienceDirect

Bone

journal homepage: www.elsevier.com/locate/bone

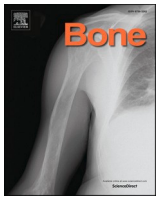

Full Length Article

A novel deletion involving the first *GNAS* exon encoding Gsα causes PHP1A without methylation changes at exon A/B

Devon Campbell [a,1], Monica Reyes [a,1], Sare Betul Kaygusuz [b], Saygın Abali [c], Tulay Guran [b], Abdullah Bereket [b], Masayo Kagami [d], Serap Turan [b], Harald Jüppner [a,e,*]

[a] *Endocrine Unit, Massachusetts General Hospital and Harvard Medical School, Boston, MA, USA*
[b] *Department of Pediatric Endocrinology, Marmara University School of Medicine, Istanbul, Turkey*
[c] *Department of Pediatric Endocrinology, Acibadem Mehmet Ali Aydinlar University School of Medicine, Istanbul, Turkey*
[d] *Department of Molecular Endocrinology, National Research Institute for Child Health and Development, Tokyo 157-8535, Japan*
[e] *Pediatric Nephrology Unit, Massachusetts General Hospital and Harvard Medical School, Boston, MA, USA*

ARTICLE INFO

Keywords:
Pseudohypoparathyroidism type Ia (PHP1A)
Albright hereditary osteodystrophy
Parathyroid hormone
Calcium
Phosphate
Gs-alpha
Gsα
Epigenetics
GNAS methylation

ABSTRACT

Individuals affected by pseudohypoparathyroidism type 1A (PHP1A) display hyperphosphatemia and hypocalcemia despite elevated PTH levels, as well as features of Albright Hereditary Osteodystrophy (AHO). PHP1A is caused by variants involving the maternal *GNAS* exons 1–13 encoding the stimulatory G protein α-subunit (Gsα). MLPA and aCGH analysis led in a male PHP1A patient to identification of a *de novo* 1284-bp deletion involving *GNAS* exon 1. This novel variant overlaps with a previously identified 1438-bp deletion in another PHP1A patient (ref. Li et al. (2020) [13], patient 2) that extends from the exon 1 promoter into the up-stream intronic region. This latter deletion is associated with reduced methylation at *GNAS* exon A/B, *i.e.* the differentially methylated region (DMR) that is demethylated in most pseudohypoparathyroidism type 1B (PHP1B) patients. In contrast, genomic DNA from our patient revealed no evidence for an epigenetic *GNAS* defect as determined by MS-MLPA and pyrosequencing. These findings thus reduce the region, which, in addition to other nucleotide sequences telomeric of exon A/B, may undergo histone modifications or interacts with transcription factors and possibly as-yet unknown proteins that are required for establishing the maternal methylation imprints at this site. Taken together, nucleotide deletions or changes within an approximately 1300-bp region telomeric of exon A/B could be a cause of PHP1B variants with complete or incomplete loss-of-methylation at the exon A/B DMR. In addition, when investigating patients with suspected PHP1A, MLPA should be considered to search for structural abnormalities within this difficult to analyze genomic region comprising *GNAS* exon 1.

1. Introduction

The term pseudohypoparathyroidism (PHP) was first introduced by Fuller Albright and colleagues when describing several patients who presented with hypocalcemia and hyperphosphatemia [1]. In addition, these and subsequent cases showed clinical features, now referred to as Albright hereditary osteodystrophy (AHO), that include early-onset obesity, short stature, brachydactyly, and various degrees of neurocognitive impairment. The mineral ion abnormalities in these patients are associated with resistance to parathyroid hormone (PTH) rather than hormonal deficiency and such cases were later shown to have impaired PTH-stimulated cAMP generation in the proximal renal tubules and thus much reduced or absent urinary cAMP and phosphate excretion [2]. Subsequently, other patients with similar clinical and laboratory features revealed elevated PTH and frequently elevated TSH levels, and hormonal resistance was shown to be associated with an approximately 50% reduction in G protein activity in readily accessible tissues [3–6]. Based on the latter findings, this disorder is now referred to as PHP type Ia (PHP1A). PHP1A is caused by mutations involving the maternal *GNAS* exons 1–13 that encode Gsα, while the same or similar mutations on the paternal allele are responsible for pseudo-PHP (PPHP) [6–9]. In contrast, PHP patients with normal G protein activity yet similar biochemical abnormalities, in most cases without AHO features, were classified as being affected by PHP type Ib (PHP1B) [6,10,11].

* Corresponding author at: Endocrine Unit, Massachusetts General Hospital and Harvard Medical School, Boston, MA, USA.
E-mail address: hjueppner@partners.org (H. Jüppner).
[1] Contributed equally.

https://doi.org/10.1016/j.bone.2022.116344
Received 19 December 2021; Received in revised form 17 January 2022; Accepted 25 January 2022
Available online 29 January 2022

Besides Gsα, the *GNAS* locus gives rise to several additional transcripts, which are generated through the use of alternative first exons that splice onto *GNAS* exons 2–13. Three of these alternative first exons, including exon A/B, are methylated on the maternal allele, while exon NESP is methylated on the paternal *GNAS* allele [6,11,12]. The inherited forms of PHP1B are caused by different deletions, duplications, or an inversion involving maternal *STX16* or *GNAS*, which lead to loss-of-methylation at one or all three differentially methylated *GNAS* regions. Genomic DNA from sporadic PHP1B patients show abnormal epigenetic changes at all four differentially methylated regions (DMRs), yet this most frequent variant of PHP1B remains genetically unresolved, except for cases of patUPD20q [6,11].

Recently, Li et al. described a male patient affected by PHP1A, whose disorder is caused by a maternally inherited, apparently 1438-bp deletion comprising most of the *GNAS* exon 1 promoter and more than 1000 bp of the up-stream centromeric intron; this deletion is associated with an incomplete loss-of-methylation at *GNAS* exon A/B ([13]; patient 2). In contrast, another PHP1A patient with a 2015-bp deletion that comprises the entire exon 1, a small portion of the up-stream intron, and more than 1300 intronic nucleotides telomeric of exon 1 revealed no evidence for abnormal *GNAS* methylation [14]. This suggests that methylation at the exon A/B DMR requires intronic sequence downstream of this exon for interaction with an as-yet unknown protein(s) that facilitates epigenetic changes directly or indirectly.

We now describe a male patient, 262/II-1, who presented with severe hypocalcemia and hyperphosphatemia despite substantially increased PTH, an elevated TSH level, and brachydactyly and obesity as his most obvious AHO features. A novel deletion of the entire *GNAS* exon 1 and the adjacent introns was identified thus establishing the diagnosis of PHP1A; this deletion was not identified in the unaffected parents and brother. No methylation changes at exon A/B were observed, thereby defining further the *GNAS* region that is required for facilitating methylation at this maternal DMR.

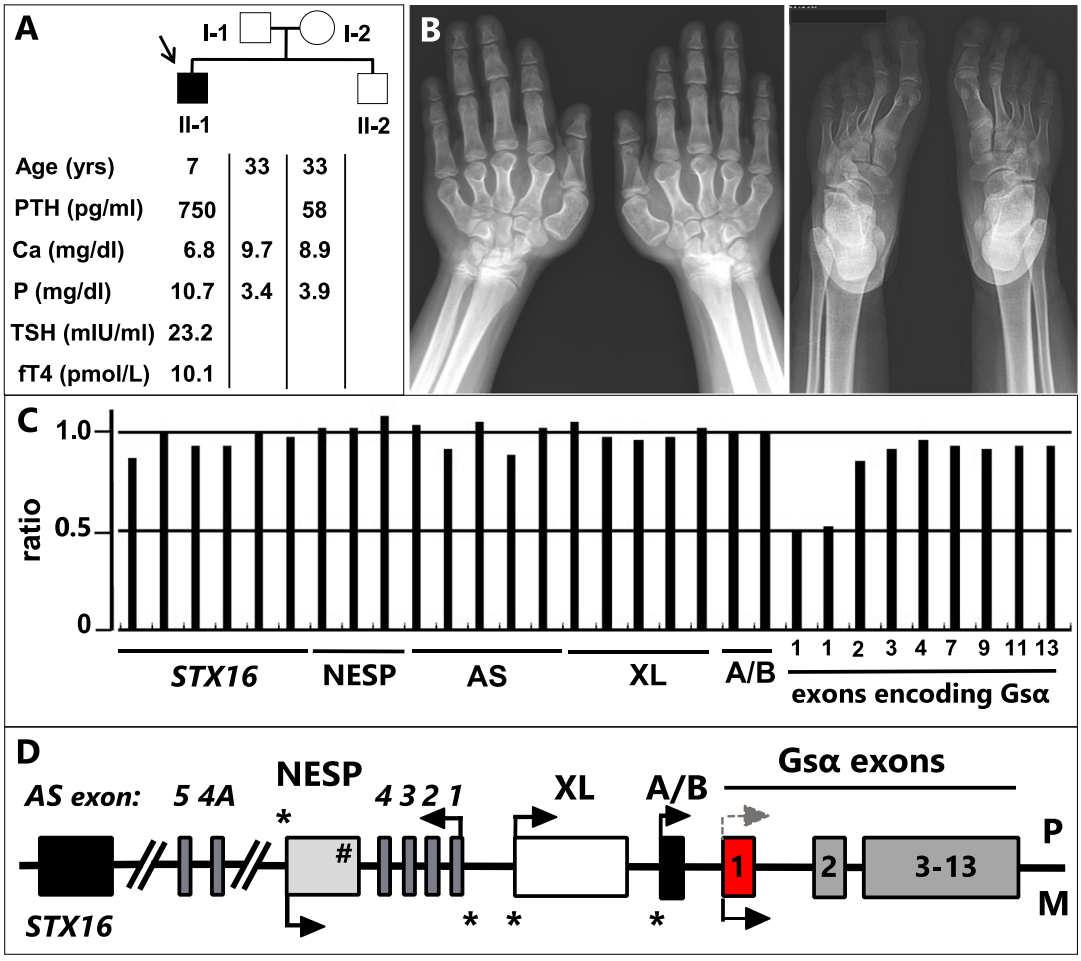

Fig. 1. Investigations of patient 262/II-1 and his family.
Panel A: Pedigree and laboratory measurements (patient: filled square and black arrow; father and brother, open square; mother open circle).
Panel B: Radiographs of the patient's hands (left) and feet (right) at the age of 11 years.
Panel C: MPLA for the *STX16* and *GNAS* region using genomic DNA from patient 262/II-1, which revealed loss of one copy of exon 1.
Panel D: Schematic representation of the region between *STX16* and *GNAS*, exon 1 is shown in red because of the heterozygous deletion identified in presented patient. *GNAS* gives rise to several imprinted sense and an antisense (AS) transcripts, including Gsα (encoded by exons 1 through 13). Gsα is mostly biallelically expressed, except for the proximal renal tubules and a few other tissues/cells in which paternal Gsα expression is partially or completely silenced (gray arrow). The alternative first exons XL and A/B splice onto exons 2 through 13 thus giving rise to the extra-large XLαs protein and the A/B transcript. Exon NESP, encoding a neuroendocrine secretory peptide, splices also onto exons 2 through 13, although translation does not extend beyond the termination codon in this exon (#). Several differentially methylated regions (DMRs) within the alternative first exons of *GNAS* undergo parent-specific methylation (asterisks), thus restricting transcription to either the maternal allele (NESP) or the paternal allele (A/B, XL, and AS). The promoter driving expression of Gsα does not undergo parent-specific methylation. (For interpretation of the references to colour in this figure legend, the reader is referred to the web version of this article.)

2. Materials and methods

2.1. Patient

A 7 year-old boy presented with seizures to a local emergency room before transfer to Marmara University for further evaluations. Laboratory studies revealed hypocalcemia (6.8 mg/dl), hyperphosphatemia (10.7 mg/dl), a considerably elevated PTH level (753 pg/ml) and a low 25-OH vitamin D level (13.3 ng/ml). TSH was 23.2 μIU/ml (normal: 0.34–5.6), fT4 10.1 pmol/l (normal: 8.4–13.6) (Fig. 1A). There was no evidence for anti-thyroid antibodies, calcitonin was 10.3 pg/ml (normal: ≤11.5), and uric acid was 2.3 mg/dl (normal: 3.5–7.2). The patient's height was 121.7 cm (+0.5 SDS), weight was 31.1 kg (+2.1 SDS), BMI was 21 kg/m^2 (+2.4 SDS); growth hormone stimulation tests revealed a maximal peak of 8.8 and 7.7 mg/dl after clonidine and L-dopa administration, respectively (normal: peak above 7 ng/ml). All metacarpals and most metatarsals are short (Fig. 1B), but there is no evidence for ectopic ossifications. The laboratory measurements along with the physical findings were consistent with PHP and treatment with calcitriol, oral calcium and L-thyroxin was therefore initiated.

At birth, the patient's weight had been 3.0 kg with a length of 49 cm, no abnormalities were observed in the neonatal screen. Father and brother are both unaffected and show no evidence for AHO; the mother's height is 157 cm (−1.09 SDS), her weight before her pregnancies was 55–56 kg; she revealed no evidence for AHO, *i.e.* no round face, no ectopic ossifications, and no brachydactyly. Both parents showed no laboratory evidence for hypocalcemia or hyperphosphatemia (see Fig. 1A), but low 25-OH vitamin D levels of 10.6 ng/ml (father) and 16.1 ng/ml (mother).

On follow-up, the patient grew along the 50th percentile. His pubertal development started relatively early at 9 years of age when his testicular volumes were 4 ml; the bone age was advanced by 2 years. At that time, his growth velocity increased and his height reached the 75th percentile. The last examination at the age of 11.3 years revealed height, weight and BMI of 130 cm (+1.2 SDS), 57.6 kg (+2.0 SDS), and 25.6 kg/m^2 (+1.9 SDS), respectively; he was Tanner stage IV with testicular volumes of 12 ml. His target height was calculated to be −0.64 SDS.

Informed written consent or assent was obtained from the patient, parents and brother using forms approved by the Institutional Review Board (IRB) of the Massachusetts General Hospital.

2.2. Multiplex Ligation-dependent Probe Amplification (MLPA), Methylation-Specific MLPA (MS-MLPA), and Polymerase Chain Reaction (PCR)

Genomic DNA was extracted from EDTA blood samples using standard techniques. MLPA and MS-MLPA were performed using the ME031-B2-GNAS kit (MRC-Holland, Amsterdam, Netherland: https://www.mlpa.com/) following the instructions provided by the manufacturer and as described [15,16]. After confirming by gel electrophoresis that DNA bands of the expected size had been amplified, analyses of the PCR products were performed at the DNA Core Facility of the Massachusetts General Hospital using an ABI3130 genetic analyzer with GeneMapper analysis software (Applied Biosystems). To analyze SNPs rs12481574 and rs55830103, and to assess the extent of the exon 1 deletion, several different forward and reverse primers were used (Suppl. Tables S1-S5).

2.3. GNAS nucleotide sequence analysis

Nucleotide sequence analysis of all *GNAS* exons and exon-intron boundaries was performed by Sanger sequencing using genomic DNA isolated from peripheral blood (Diagnostic Center for Genetic Diseases, Haseki Research and Education Hospital, Istanbul, Turkey). However, no evidence for a disease-causing variant was obtained; note that no heterozygous polymorphism was identified in exon 1 when analyzing the genomic DNA of patient 262/II-1. The heterozygous c.1127C>T change in exon XL that changes proline to leucine (p.P376L) is a known polymorphism rs61749697 (data not shown), which is unlikely to cause the patient's clinical and laboratory findings.

2.4. Methylation analysis using pyrosequencing

Methylation analysis of the *GNAS* locus was also conducted by pyrosequencing with PyroMark Q24 (Qiagen), as previously reported [17], to assess six CpG sites at *GNAS-NESP*:TSS-DMR, six CpG sites at *GNAS-AS1*:TSS-DMR, seven CpG sites at *GNAS-XL*:Ex1-DMR, and seven CpG sites at *GNAS A/B*:TSS-DMR. Primer sets utilized in this study are shown in Suppl. Table S6.

2.5. Array-based Comparative Genomic Hybridization (aCGH)

We conducted array-based comparative genomic hybridization (aCGH) analysis using a custom-built array (4 × 180K format, Design ID 032112, Agilent Technologies, Palo Alto, CA, USA). The procedure was performed as described in the manufacturer's instructions and as recently reported [17,18].

3. Results

Initial laboratory studies for patient 262/II-1, but not his parents, had shown severe hypocalcemia and hyperphosphatemia as well as a profound PTH elevation (Fig. 1A). In addition, some AHO features were observed, including shortening of all metacarpals and of metatarsals 3 to 5 (Fig. 1B). MLPA was performed because nucleotide sequence analysis of *GNAS* had revealed no evidence for a disease-causing variant involving exons 1–13, and because the clinical and radiographic findings observed in our patient can be encountered in some PHP1B cases [6,19]. These studies provided evidence for a deletion restricted to *GNAS* exon 1 (probes 03883-L23597 and 03884-L22605) (Fig. 1C, D), which was confirmed with the only two aCGH probes in that region, namely A_16_P22459497 and A_16_P21174375 (Fig. 2A). There was no evidence for abnormal methylation at the four *GNAS* DMRs as determined by MS-MLPA (data not shown) and by pyrosequence analysis that included the exon A/B DMR (nucleotides 57,463,265 to 57,465,201; GRCh37/hg19) [20], which was targeted by a primer set interrogating the 57,463,531 to 57,463,746 region. Consistent with the MS-MLPA data (Fig. 1C), no methylation changes were observed by pyrosequence analysis at the three other *GNAS* DMRs (Fig. 2B). These findings indicated that patient 262/II-1 has a heterozygous deletion comprising the first exon encoding Gsα and that this variant does not cause epigenetic *GNAS* changes.

Analysis of the patient's genomic DNA revealed that SNP rs55830103 up-stream of exon 1 is homozygous and thus uninformative (Fig. 3A), but aCGH analysis with probe A_16_P55120906 (chr20: 57,465,637 to 57,465,681) provided no evidence for a deletion (see Fig. 2A). In contrast, probe A_16_P22459497 (chr20:57,465,955 to 57,465,999) revealed a reduction in copy number, thus suggesting that the centromeric boundary of the deletion is located between A_16_P55120906 and A_16_P22459497. However, MLPA and aCGH analysis made it unlikely that the deletion in patient 262/II-1 extends as far centromeric of *GNAS* exon 1 as the deletion reported by Li et al. for patient 2 [13] (see Figs. 1C and 2A).

Another SNP, rs12481574 (chr20:57,468,807), located between *GNAS* exons 1 and 2, is heterozygous A/G indicating that the telomeric breakpoint for the presumed deletion in 262/II-1 is located between rs12481574 and *GNAS* exon 1 (Fig. 3A, B). Our patient's genomic DNA revealed normal methylation at the exon A/B DMR as determined by MS-MLPA (not shown) and pyrosequencing (see Fig. 2B), thus making it likely that the centromeric breakpoint of the deletion is located within a region of approximately 1000 nucleotides up-stream of exon 1 (Fig. 3A). These findings are different from those for patient 2 in the report by Li

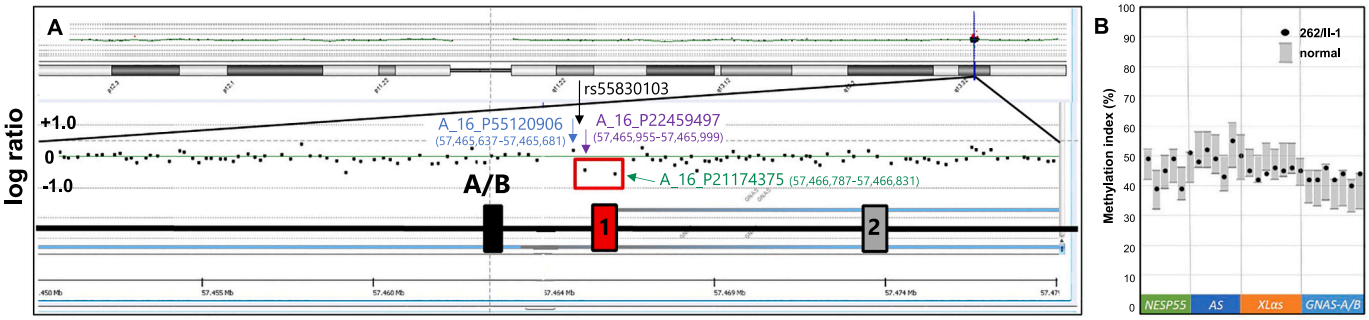

Fig. 2. Analysis of genomic DNA from patient 262/II-1 by aCGH and pyrosequencing.
Panel A: Depiction of portions of the *GNAS* region including exon A/B, and the first two exons encoding Gsα; exon 1 (red) is deleted from one parental allele. The aCGH probes are indicated by black dots; the two probes (A_16_P22459497, purple arrow and font; A_16_P21174375, green arrow and font) confirming deletion of exon 1 and the surrounding region are high-lighted by a red box. Probe A_16_P55120906 (blue arrow and font) and location of SNP rs55830103 (black arrow and font) are also shown. All coordinates are based on the GRCh37/hg19 assembly.
Panel B: Analysis of the four DMRs within the *GNAS* region by pyrosequencing. Methylation at the different sites for unaffected controls is indicated by gray boxes; for patient 262/II-1 methylation at each site is indicated by black circles. No evidence was obtained for abnormal methylation at the different *GNAS* DMRs. (For interpretation of the references to colour in this figure legend, the reader is referred to the web version of this article.)

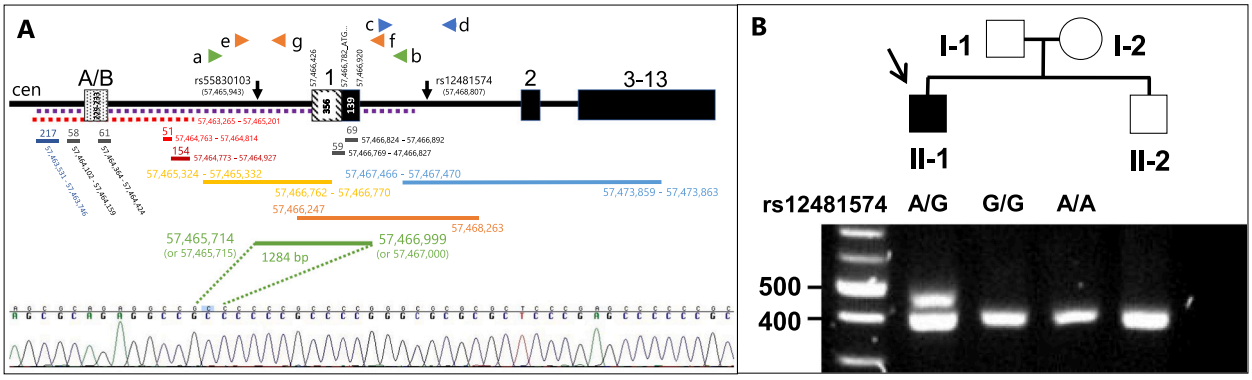

Fig. 3. Depiction of the investigated *GNAS* locus, the location of the four genetically defined deletions and of the probes and primers that allowed determination of the molecular defect in PHP1A patient 262/II-1.
Panel A: Schematic representation of the *GNAS* region between exon A/B (stippled box, 229 bp) and exons encoding Gsα (black boxes) (all coordinates based on GRCh37/hg19). The green horizontal bar represents the deletion of 1284 bp identified in 262/II-1, which includes the entire exon 1 (nucleotides 57,466,426 to 57,466,920; non-coding, striped box of 357 bp; the coding region starts with the initiator methionine, black box of 139 bp) as well as adjacent intronic sequences (thick black horizontal line). SNP rs12481574 was found to be heterozygous A/G for the patient, while the father is G/G and the mother is A/A (see Panel B). Approximate locations of primers used allowing identification of the deletion are shown by differently colored triangles and their identifying letters (sequences of primers and the expected sizes of the PCR products are shown in Suppl. Table 1). The purple dashed line indicates a CpG-rich region as provided by the UCSC Genome Browser (nucleotides 57,463,653 to 57,467,739); the red dashed line indicates the exon A/B DMR [20]. Deletions and approximate breakpoints that were reported for other PHP1A patients are depicted with yellow and blue horizontal lines [13] or with an orange horizontal line [14]. The dark red line (154 bp) represents the most telomeric region affecting methylation of the exon A/B DMR on chromosome 20 as defined by the Genetics Laboratory at CHOP and the red line (51 bp) represents the most telomeric region affecting methylation of the exon A/B DMR as defined by the Genetics Laboratory at John Hopkins University [13]. The dark blue line (217 bp) represents data obtained by pyrosequencing, see Fig. 2B. The gray lines (58 and 61 bp) represent the two different MLPA probes (06191-L23094 and 03882-L22603) used for evaluation of methylation changes at exon A/B; cen, centromeric.
Panel B: Pedigree of family 262 and genotype analysis for SNP rs12481574 of patient 262/II-1 and his parents (patient: filled square and black arrow; father and brother, open square; mother open circle). Multiplex PCR led to amplification of an approximately 400 bp band, which is derived from the wild-type allele, when using primers **e** and **g** with DNA from 262/II-1 and his unaffected parents and brother. A DNA band between the 400-bp and 500-bp size markers was amplified with primers **e** and **f**, but only when using the patient's DNA. A 3% agarose gel was used for electrophoresis; the 100-bp ladder is shown on the left. (For interpretation of the references to colour in this figure legend, the reader is referred to the web version of this article.)

et al. [13], which had shown a significant loss-of-methylation at exon A/B in association with a deletion that extends from the promoter portion of exon 1 to nucleotide 57,465,324 (see Fig. 3A, yellow bar). Thus although no heterozygous SNPs could be identified up-stream exon 1, the lack of epigenetic changes in 262/II-1 made it likely that the centromeric breakpoint of the deletion is located less than 800 bp up-stream of *GNAS* exon 1.

To determine the telomeric breakpoint of the deleted region, forward primer **c** and reverse primer **d** were used to amplify across rs12481574. Nucleotide sequence analysis revealed that patient 262/II-1 is heterozygous A/G for this SNP (see Fig. 3B) indicating that the telomeric breakpoint of the deletion is not located within the 1786 bp region extending from 57,467,565 to 57,469,350 (GRCh37/hg19). We therefore generated reverse primer **b** that is located closer to exon 1 than reverse primer **d**, but within the region comprising both parental alleles, which was used for PCR amplification in combination with several different forward primers up-stream of exon 1. When using forward primer **a** and reverse primer **b**, a single DNA band of approximal 800 bp was amplified, which is much smaller than the expected size of 2195 bp (not shown). Nucleotide sequence analysis of this PCR product revealed the expected nucleotide sequences at the 5′ and the 3′ end, yet a 1284-bp deletion extending from nucleotides 57,465,714 to 57,466,999 (or from

57,465,715 to 57,467,000 depending on the location of a single cytosine).

To confirm heterozygosity for this deletion, a multiplex PCR was performed using the forward primer **e** upstream of exon 1 and two different reverse primers, namely primer **g** located within the deleted region and primer **f** located downstream outside of the deleted region. The PCR amplicon for the wild-type allele using forward primer **e** and reverse primer **g** was expected to be 399 bp in length, while the amplicon when using reverse primer **f** was expected to amplify 470 bp for the allele with the deletion. Our multiplex PCR revealed for patient 262/II-1 a strong band of approximately 400 bp, in addition to another band between the 400-bp and 500-bp size markers. Only the approximately 400-bp band, but not the band between the 400-bp and 500-bp marker, was amplified when using genomic DNA from both parents and from the unaffected sibling (see Fig. 1A). Nucleotide sequence analysis of the 400-bp band revealed the expected wild-type sequence at the 5′ and the 3′ ends, and analysis of the larger band confirmed the deletion of 471 bp between nucleotides 57,465,714 to 57,466,999 (or 57,465,715 to 57,467,000). On the other hand, the approximately 400-bp band amplified from both parents and from the unaffected brother revealed the wild-type sequence of 399 bp, indicating that the patient's deletion had most likely occurred *de novo*.

4. Discussion

In a patient with clinical AHO features and clear evidence for PTH-resistant hypocalcemia and hyperphosphatemia as well as an elevated TSH level, we identified a novel deletion involving *GNAS* exon 1, which is only the fourth intragenic mutation involving this exon as a cause of PHP1A. Given the number of repetitive sequences in this GC-rich portion of *GNAS*, only two aCGH probes had been established for this region [17,18], which confirmed the deletion initially detected by MLPA. However, aCGH analysis alone might have failed to provide convincing evidence for the deletion. Consequently, MLPA should be considered for identification of structural abnormalities within this *GNAS* region that is difficult to analyze. As for the other similarly sized deletions within this locus [13,14], there is no evidence for a direct repeat sequence adjacent to both breakpoints making it uncertain which mechanism could have led to the deletion.

The identified deletion, which removes the entire exon 1 and adjacent intronic sequences, most likely occurred *de novo* because both parents, who are unaffected, revealed no evidence for the same genetic variant. It appears very likely that the mutation had occurred on the maternal allele because obvious mineral ion abnormalities as well as elevated PTH and TSH levels were observed when the patient was first evaluated for seizures. Unlike the deletion described by Li et al. ([13] patient 2), genomic DNA from our patient showed no evidence for epigenetic changes at *GNAS* exon A/B, as determine by MS-MLPA and pyrosequence analysis, which is identical to our previous findings in another PHP1A patient with a larger deletion involving exon 1 [14], but the centromeric breakpoint of that case is located further telomeric than in patient 262/II-1. Given the lack of epigenetic changes, the deletion identified in 262/II-1 reduces to approximately 400 bp the region involved in facilitating, directly or indirectly, interactions with a methyltransferase that is required for establishing the parent-specific epigenetic changes at exon A/B. In fact, these nucleotides with regulatory function are presumably located outside of or immediately adjacent to the portion of the CpG island at exon A/B that undergoes differential methylation, and may comprise sites for histone modifications or for interaction with transcription factors or possibly as-yet unknown proteins required for establishing methylation at this site. It is therefore conceivable that genetic variants telomeric of the maternal *GNAS* exon A/B or defects in proteins that interact with this genomic region could lead to PHP1B variants by reducing or abolishing exon A/B methylation.

CRediT authorship contribution statement

Devon Campbell and Monica Reyes designed and performed MS-MLPA, MLPA, all PCRs, and nucleotide sequence analyses, and both helped revise the final draft of the manuscript.

Devon Campbell wrote the first draft of the manuscript and generated the first draft of all figures and of supplemental tables 1–5.

Sare Betul Kaygusuz, Saygın Abali, Tulay Guran, Abdullah Bereket, and Serap Turan performed all clinical and laboratory investigations.

Masayo Kagami performed pyrosequence analysis and array-based CGH, provided supplemental table 6, and edited the manuscript.

Harald Jüppner revised all figures and tables, and generated the final draft of the manuscript.

Acknowledgements

We would like to thank the patient and his family for participating in this study as well as Anjali Vlassak for her contribution to the initial experiments to define the underlying genetic defect in 262/II-1. The authors have no conflict of interest. This work was supported by NIH grants RO1-DK46718 and PO1-DK11794 (subproject III) (HJ) and Supplement Funds DK236464 (HJ, DC).

Appendix A. Supplementary data

Supplementary data to this article can be found online at https://doi.org/10.1016/j.bone.2022.116344.

References

[1] F. Albright, C.H. Burnett, P.H. Smith, W. Parson, Pseudohypoparathyroidism - an example of "seabright-bantam syndrome", Endocrinology 30 (1942) 922–932.
[2] L.R. Chase, G.L. Melson, G.D. Aurbach, Pseudohypoparathyroidism: defective excretion of 3',5'-AMP in response to parathyroid hormone, J. Clin. Invest. 48 (10) (1969) 1832–1844.
[3] A.H. Tashjian Jr., A.G. Frantz, J.B. Lee, Pseudohypoparathyroidism: assays of parathyroid hormone and thyrocalcitonin, Proc. Natl. Acad. Sci. U. S. A. 56 (1966) 1138–1142.
[4] Z. Farfel, A.S. Brickman, H.R. Kaslow, V.M. Brothers, H.R. Bourne, Defect of receptor-cyclase coupling protein in pseudohypoparathyroidism, N. Engl. J. Med. 303 (1980) 237–242.
[5] M.A. Levine, R.W. Downs Jr., M. Singer, S.J. Marx, G.D. Aurbach, A.M. Spiegel, Deficient activity of guanine nucleotide regulatory protein in erythrocytes from patients with pseudohypoparathyroidism, Biochem. Biophys. Res. Commun. 94 (4) (1980) 1319–1324.
[6] G. Mantovani, M. Bastepe, D. Monk, et al., Diagnosis and management of pseudohypoparathyroidism and related disorders: first international consensus statement, Nat Rev Endocrinol. 14 (8) (2018) 476–500.
[7] L.S. Weinstein, P.V. Gejman, E. Friedman, et al., Mutations of the gs a-subunit gene in albright hereditary osteodystrophy detected by denaturing gradient gel electrophoresis, Proc. Natl. Acad. Sci. U. S. A. 87 (1990) 8287–8290.
[8] J.L. Patten, D.R. Johns, D. Valle, et al., Mutation in the gene encoding the stimulatory G protein of adenylate cyclase in Albright's hereditary osteodystrophy, N. Engl. J. Med. 322 (20) (1990) 1412–1419.
[9] S.J. Davies, H.E. Hughes, Imprinting in Albright's hereditary osteodystrophy, J. Med. Genet. 30 (1993) 101–103.
[10] M. Levine, Hypoparathyroidism and pseudohypoparathyroidism, in: DeGroot L. J. JJ (Ed.), Endocrinology, Fifth edition 2, W.B. Saunders Co, Philadelphia, PA, 2005, pp. 1611–1636.
[11] H. Jüppner, Molecular definition of pseudohypoparathyroidism variants, J. Clin. Endocrinol. Metab. 106 (6) (2021) 1541–1552.
[12] J. Danzig, D. Li, S. Jan de Beur, M.A. Levine, High-throughput molecular analysis of pseudohypoparathyroidism 1b patients reveals novel genetic and epigenetic defects, J. Clin. Endocrinol. Metab. 106 (11) (2021) e4603–e4620.
[13] D. Li, C. Bupp, M.E. March, H. Hakonarson, M.A. Levine, Intragenic deletions of GNAS in pseudohypoparathyroidism type 1A identify a new region affecting methylation of exon A/B, J. Clin. Endocrinol. Metab. 105 (9) (2020).
[14] M. Reyes, A. Karaca, M. Bastepe, N.E. Gulcelik, H. Jüppner, A novel deletion involving GNAS exon 1 causes PHP1A and further refines the region required for normal methylation at exon A/B, Bone 103 (2017) 281–286.
[15] R. Takatani, A. Molinaro, G. Grigelioniene, et al., Analysis of multiple families with single individuals affected by pseudohypoparathyroidism type ib (PHP1B) reveals only one novel maternally inherited GNAS deletion, J. Bone Miner. Res. 31 (2016) 796–805.
[16] P. Loid, M. Pekkinen, M. Reyes, et al., GNAS, PDE4D, and PRKAR1A mutations and GNAS methylation changes are not a common cause of isolated early-onset severe obesity among Finnish children, Front. Pediatr. 8 (2020) 145.

[17] A. Nakamura, E. Hamaguchi, R. Horikawa, et al., Complex genomic rearrangement within the GNAS region associated with familial pseudohypoparathyroidism type 1b, J. Clin. Endocrinol. Metab. 101 (7) (2016) 2623–2627.
[18] M. Reyes, M. Kagami, S. Kawashima, et al., A novel GNAS duplication associated with loss-of-methylation restricted to exon A/B causes pseudohypoparathyroidism type Ib (PHP1B), J. Bone Miner. Res. 36 (3) (2021) 546–552.
[19] F.M. Elli, L. de Sanctis, V. Bollati, et al., Quantitative analysis of methylation defects and correlation with clinical characteristics in patients with pseudohypoparathyroidism type I and GNAS epigenetic alterations, J. Clin. Endocrinol. Metab. 99 (3) (2014) E508–E517.
[20] D. Monk, J. Morales, J.T. den Dunnen, et al., Recommendations for a nomenclature system for reporting methylation aberrations in imprinted domains, Epigenetics. 13 (2) (2018) 117–121.